THE JOURNAL OF PHYSICAL CHEMISTRY A

Article

Cite This: J. Phys. Chem. A 2019, 123, 5428−5435

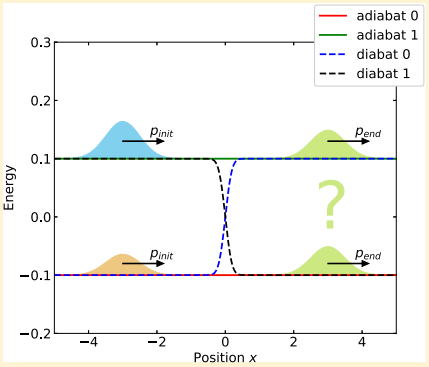
pubs.acs.org/JPCA

Revisiting the Recoherence Problem in the Fewest Switches Surface Hopping Algorithm

Gaohan Miao* and Joseph Subotnik

Department of Chemistry, University of Pennsylvania, Philadelphia, Pennsylvania 19104, United States

ABSTRACT: We isolate and dissect exactly how and why Tully's fewest switches surface hopping (FSSH) algorithm fails when two wave packets come together at a crossing and "recohere". Using two different one-dimensional avoided crossing models and an initial wave function, which is a superposition of wave packets on different adiabats, we show that the key failures pertain to asymptotic nuclear momenta rather than electronic populations. Moreover, these FSSH failures stem from the fundamental assumption of independent trajectories with time-local hopping. As such, there is no possible means to correct FSSH without either (i) introducing time-nonlocal dynamics (i.e., allowing trajectories to move forward and backward in time) or (ii) requiring that trajectories interact.



Downloaded via UNIV OF PENNSYLVANIA on July 31, 2019 at 15:00:21 (UTC).
See https://pubs.acs.org/sharingguidelines for options on how to legitimately share published articles.

1. INTRODUCTION

As proposed by Tully in 1990,[1] the fewest switches surface hopping (FSSH) algorithm has been widely applied to simulate a host of different experimentally relevant phenomena,[2−11] which all fall under the title nonadiabatic dynamics—dynamics where the nuclear motion and electronic motion are highly entangled and the Born−Oppenheimer approximation breaks down. The success of the FSSH semiclassical algorithm arises primarily from FSSH's practical ability to achieve reasonably accurate results[12−14] with only a minimal cost to implement.[1,15,16] And yet, despite its advantages, FSSH has several well-known shortcomings. For instance, standard FSSH fails to correctly treat the separation of one wave packet into two wave packets that separate one from the other—this is the well-known decoherence problem. The decoherence problem has been investigated by many researchers over the past 3 decades (going back to Rossky,[17−19] Truhlar,[20−23] and Hammes-Schiffer[7,24]), and the signatures of decoherence failures are spurious resonances arising when fictitious wave packets recombine.[9,25,26] Today, the decoherence anomalies can be largely fixed by some modified versions of the FSSH algorithm,[17,18,20−24,26−28] and the decoherence problem can be tied back to a rigorous quantum classical Liouville equation (QCLE).[29,30]

Now, apart from the decoherence problem, FSSH also suffers from the so-called "recoherence" problem for surface hopping: FSSH is unable to successfully simulate the merging of two well-separated wave packets that come together at a crossing. While such a surreptitious event may seem unlikely when simulating photochemical branching following a pulse of light, the recoherence problem clearly becomes relevant when simulating dipole−dipole correlation functions for spectroscopy: one must initialize simulations with coherences, which oscillate between the ground and excited states, and then propagate such coherences. It is well known in the literature that, when propagating coherences, Ehrenfest dynamics often does better than surface hopping,[31,32] though the exact reasoning behind this statement is not always clear. As far as the recoherence problem is concerned, the physics underlying the surface hopping dynamics is not very clear: when is recoherence a problem? What is the signature of recoherence? What are the exact failures? These diagnostic and fundamental questions have not been fully explained.[9,33]

In this paper, our goal is to revisit these specific FSSH recoherence problems. Using two simple one-dimensional (1D) scattering models, we will show that the key FSSH failure is the inability to predict the correct momenta (and not electronic populations) when two wave packets recombine at a region of nonadiabatic coupling. We will also show that this recoherence failure cannot be corrected with any simple phase correction[34] but is rather a fundamental limitation of Tully's ansatz of noninteracting trajectories (with Markovian dynamics and too much hopping back and forth between surfaces). Thus, in the end, this manuscript can be used to understand both when and why surface hopping fails, and, perhaps, our conclusions here will lead to improved stochastic nonadiabatic dynamic protocols in the future.

This paper is structured as follows: in Section 2, we review the two basic semiclassical algorithms (FSSH and Ehrenfest). In Section 3, we introduce two model problems and present results for the different algorithms, isolating the signatures of recoherence. In Section 4, we interpret the FSSH results in terms of a "truly minimal hopping" ansatz (in the spirit of Landau−Zener theory), whereby the recoherence problem can

Received: April 5, 2019
Revised: June 8, 2019
Published: June 10, 2019

© 2019 American Chemical Society

DOI: 10.1021/acs.jpca.9b03188
J. Phys. Chem. A 2019, 123, 5428−5435

be reduced to a tractable problem, even though such an approach is not easily compatible within the FSSH framework. In Section 5, we conclude and outline future directions.

2. METHODS

For the purposes of this paper, we need to investigate only the two most basic semiclassical algorithms: (i) the FSSH algorithm and (ii) the Ehrenfest algorithm. For both approaches, a swarm of trajectories is initialized with a predetermined position and momentum distribution. Below, we will need to perform simulations where the initial state is a superposition of nuclear wave packets on different adiabats. Because this initialization requirement is not common for most FSSH simulations, a few words of introduction and review are now appropriate. To keep our notation as simple as possible and avoid multiple indices, we will assume that all dynamics are in 1D. For a more complete description, many references are available.[5,15,35]

2.1. Standard FSSH Algorithm. For FSSH simulations, each trajectory is assigned a set of predetermined quantum amplitudes $(c_0, c_1, ..., c_{N-1})^T$, which are the coordinates of the electronic wave function in the basis of adiabatic states $\{|\phi_0\rangle, |\phi_1\rangle, ..., |\phi_{N-1}\rangle\}$: $|\psi_{el}\rangle = \sum_i c_i|\phi_i\rangle$. A single trajectory with these coefficients is assigned to one adiabatic surface $\{0, 1, ..., N-1\}$ with probability $\{|c_0^2, |c_1|^2, ..., |c_{N-1}|^2\}$, respectively. This initialization scheme is consistent with quasi-derivations of the FSSH algorithm starting with the quantum classical Liouville equation (QCLE).[29,30]

After initialization, according to FSSH, each trajectory is propagated along its active adiabatic surface (which is denoted as j). The nucleus with position x and momentum p evolves according to Newton's laws; the electronic wave function is evolved according to the Schrödinger equation

$$\begin{aligned} \dot{x} &= \frac{p}{m} \\ \dot{p} &= -\partial_x E_j(x) \\ \dot{c}_k &= -\frac{iE_k(x)}{\hbar}c_k - \sum_{l=0}^{N-1}\frac{p}{m}d_{kl}c_l \end{aligned} \tag{1}$$

Here, $E_j(x)$ is the trajectory's current active adiabatic surface. At each time step, each trajectory can switch from its current active adiabatic surface j to a different adiabatic surface k with probability

$$P_{j\to k} = \max(..., 0)\frac{-2\Delta t \mathrm{Re}(\rho_{jk}d_{kj}p/m)}{\rho_{jj}} \tag{2}$$

Here, $\rho_{jk} \equiv c_j c_k^*$ is a density matrix element.

When a hop between two adiabats occurs, each trajectory must adjust its momentum to comply with energy conservation. In the cases where energy conservation is not possible (i.e., a trajectory does not have enough kinetic energy), the attempted hop is frustrated and the trajectory continues to move along its original adiabatic surface. In general, velocity reversal is needed if the forces on different adiabats are in opposite directions during a frustrated hop;[36] luckily, this nuance about velocity reversal will not be important here as we will work with large enough momentum such that reflection is not important.

2.1.1. Phase-Corrected FSSH. It is well known that the FSSH algorithm can fail when trajectories go through multiple crossings, wave packets separate, and decoherence is important (though neglected by Tully's original algorithm).[9,17,24] While this failure can largely be fixed with decoherence corrections, FSSH still cannot treat coherent passage of one trajectory through multiple avoided crossings.

To treat such a case, Shenvi et al. proposed modifying the propagation of the electronic wave function within FSSH.[34] The resulting phase-corrected FSSH takes into account the fact that, as trajectories are propagated on different adiabats with different effective velocities, a phase difference accumulates and the wave packets spread apart, neither of which is treated correctly by standard FSSH. According to phase-corrected FSSH, one can isolate the relative electronic phase at the position of the classical trajectory by replacing eq 1 with

$$\begin{aligned} \dot{x} &= \frac{p}{m} \\ \dot{p} &= -\partial_x E_j(x) \\ \dot{c}_k &= \frac{i}{\hbar}\frac{pp_k}{m}c_k - \sum_{l=0}^{N-1}\frac{p}{m}d_{kl}c_l \end{aligned} \tag{3}$$

Here, p_k is the momentum on adiabat k, which in the 1D case is

$$p_k = \mathrm{sgn}(p)\sqrt{p^2 + 2m[E_j(x) - E_k(x)]} \tag{4}$$

If $p^2 + 2m[E_j(x) - E_k(x)] < 0$, p_k is assigned to be 0.

For 1D model problems, refs 34 and 37 show that phase-corrected FSSH can strongly outperform standard FSSH as far as capturing electronic populations (see Figures 2 and 4 in ref 34 for trajectories going through multiple avoided crossings). In this paper, we will investigate how phase-corrected FSSH performs as far as *nuclear* observables.

2.2. Ehrenfest Algorithm. Besides FSSH, the other standard semiclassical algorithm is Ehrenfest dynamics. According to Ehrenfest dynamics, each trajectory is propagated along an average force (rather than along the force from a single adiabatic surface). This average force is[a]

$$\langle F\rangle = \mathrm{Tr}(\rho F) = -\sum_{j,k}\rho_{jk}\langle\psi_k|\partial_x H|\psi_j\rangle \tag{5}$$

Thus, Ehrenfest trajectories are propagated according to the following equations

$$\begin{aligned} \dot{x} &= \frac{p}{m} \\ \dot{p} &= \langle F\rangle \\ \dot{c}_k &= -\frac{iE_k(x)}{\hbar}c_k - \sum_{l=0}^{N-1}\frac{p}{m}d_{kl}c_l \end{aligned} \tag{6}$$

Because the Ehrenfest algorithm cannot easily predict observables in a state-refined fashion (e.g., one cannot access the nuclear momentum of one wave packet on one electronic adiabat), below, we will investigate only average Ehrenfest observables.

3. RESULTS

3.1. Model 1: Flat Adiabat with One Avoided Crossing. To begin our analysis, we first investigate a 1D model with the following Hamiltonian

DOI: 10.1021/acs.jpca.9b03188
J. Phys. Chem. A 2019, 123, 5428−5435

$$H_{\text{tot}} = -\frac{\hbar^2}{2m}\frac{\mathrm{d}^2}{\mathrm{d}x^2} + H$$

$$H = A\begin{bmatrix} -\cos\theta(x) & \sin\theta(x) \\ \sin\theta(x) & \cos\theta(x) \end{bmatrix}$$

$$\theta(x) \equiv \frac{\pi}{2}(\text{erf}(Bx) + 1) \tag{7}$$

Here, A and B are parameters (defined below), and we will investigate multiple values of A to sample the adiabatic and nonadiabatic limits. The adiabatic surfaces associated with this Hamiltonian are flat, with an avoided crossing located at $x = 0$. A schematic plot for the energy surfaces of this Hamiltonian is shown in Figure 1.

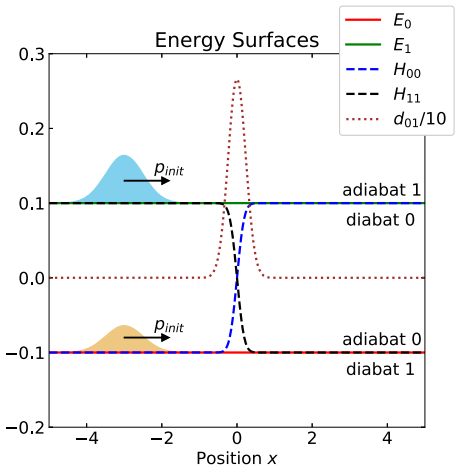


Figure 1. Energy surfaces for the Hamiltonian in eq 7. Here, $A = 0.10$, $B = 3.0$. The solid lines are adiabatic surfaces. The dashed lines are diabatic surfaces. The dotted line is the derivative coupling d_{01}. The initial Gaussian wave packets are plotted schematically with $x_{\text{init}} = -3.0$, $c_0 = 0.6$, $c_1 = 0.8$, and $\sigma = 1.0$.

At the beginning of the simulation, Gaussian wave packets are initialized on both and eq 1

$$|\Psi_0(x)\rangle = c_0\, \mathrm{e}^{ixp_{\text{init}}/\hbar}\, \mathrm{e}^{-|x-x_{\text{init}}|^2/\sigma^2}$$

$$|\Psi_1(x)\rangle = c_1\, \mathrm{e}^{ixp_{\text{init}}/\hbar}\, \mathrm{e}^{-|x-x_{\text{init}}|^2/\sigma^2} \tag{8}$$

Here, σ is a measure of the spread of the initial wave packet over real space; x_{init} and p_{init} are the initial position and momentum, respectively; and c_0 and c_1 are initialized as positive, real numbers, with $c_0^2 + c_1^2 = 1$. For exact (reference) quantum dynamics, we propagate the wave packets in eq 8 with the Schrödinger equation using the fast Fourier transform technique.[38] For semiclassical dynamics, 10^4 trajectories are sampled from the Wigner distribution corresponding to eq 8; these trajectories are propagated with either FSSH or Ehrenfest dynamics, as described in Section 2.

The scattering results for model 1 are presented in Figures 2−4. In Figure 2, we set the initial position to be $x_{\text{init}} = -3.0$, prepare the initial electronic state with $c_1^2 = 1$ (i.e., on the excited state), and scan over different p_{init}. We plot the final population on adiabat 0 and momentum on both adiabats as a function of p_{init}. For all initial momenta, both standard FSSH and phase-corrected FSSH recover the exact population and momentum quantitatively. Although not shown, Ehrenfest dynamics is equally accurate.

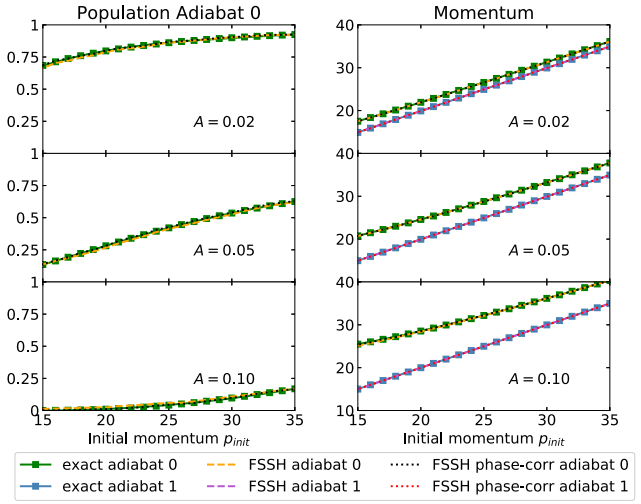


Figure 2. Results for model 1. Left: population distribution on adiabat 0 after scattering as a function of initial momentum, p_{init}. Right: the momentum on the adiabatic surfaces as a function of p_{init}. Initially, we set $c_1^2 = 1$. Both FSSH algorithms perform very well here (as does Ehrenfest, not shown).

Next, in Figures 3 and 4, we fix the initial momentum $p_{\text{init}} = 30.0$ and scan over different c_1^2. At the end of the simulation, we calculate both the average population on the lower adiabatic surface and the momentum on each adiabatic surface as a function of c_1^2; this data is plotted in Figure 3. In Figure 4, we plot the average momentum over all trajectories and all surfaces. As shown in Figure 3, while FSSH correctly recovers the exact electronic populations for different A, the FSSH momentum results are erroneous for the case $A = 0.10$. Phase-corrected FSSH results are almost the same as the FSSH results. In Figure 4, again, FSSH momentum results disagree

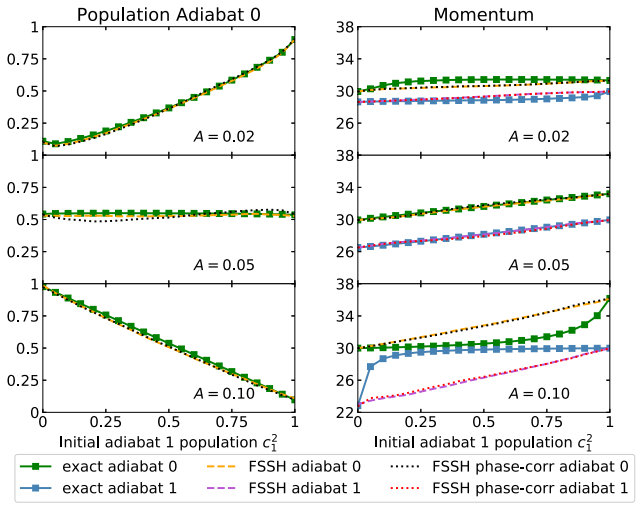


Figure 3. Results for model 1. Left: the population distribution on adiabat 0 after scattering as a function of the initial superposition factor, c_1^2. Right: the momentum on each adiabatic surface as a function of c_1^2. The initial momentum is $p_{\text{init}} = 30$. Note that FSSH always performs well for electronic population, but the momentum is incorrect for $A = 0.10$ when starting with $c_1^2 \in (0.1)$, i.e., a superposition of adiabats.

DOI: 10.1021/acs.jpca.9b03188
J. Phys. Chem. A 2019, 123, 5428−5435

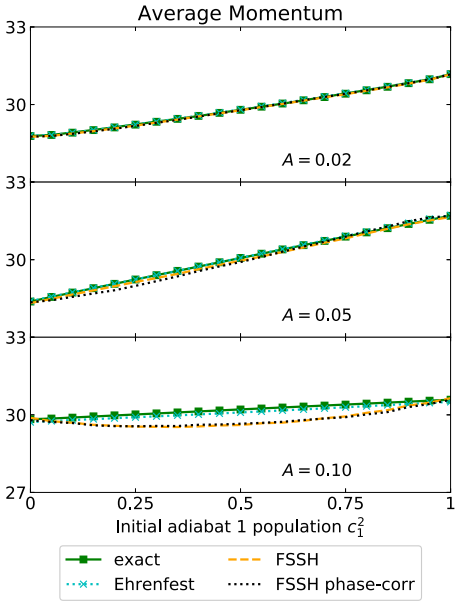


Figure 4. Results for model 1. The average momentum over all trajectories as a function of c_1^2 for the model Hamiltonian in Figure 1. The initial momentum is $p_{\text{init}} = 30$. Intriguingly, Ehrenfest dynamics strongly outperforms FSSH for the case $A = 0.10$. For this problem, the phase correction does not yield a meaningful correction to FSSH.

with the exact results when $A = 0.10$. Interestingly, however, Ehrenfest dynamics outperforms FSSH as far as momentum and do approximately recover both the correct population and momentum for all three A's.

3.2. Model 2: Flat Adiabat with Two Avoided Crossings. For our second Hamiltonian, we investigate a slightly more complex model with two avoided crossings

$$H_{\text{tot}} = -\frac{\hbar^2}{2m}\frac{\mathrm{d}^2}{\mathrm{d}x^2} + H$$

$$H = A\begin{bmatrix} -\cos\theta(x) & \sin\theta(x) \\ \sin\theta(x) & \cos\theta(x) \end{bmatrix}$$

$$\theta(x) \equiv \frac{\pi}{2}(\mathrm{erf}(B(x-C)) - \mathrm{erf}(B(x+C))) \tag{9}$$

Just as for eq 7, the adiabats are flat. However, in eq 9, we have an extra parameter C, as the Hamiltonian has two avoided crossings located at $x = -C$ and C. A schematic plot is shown in Figure 5.

Results for observables are plotted in Figure 6−8. Here, $x_{\text{init}} = -8.0$. In Figure 6, just as in Figure 2, we scan over initial momentum for dynamics initialized on the excited state (here, we also show the results of Ehrenfest dynamics). Unlike the case of model 1, we now find that, due to the accumulated phase difference between two wave packets on different surfaces, standard FSSH cannot recover the correct electronic populations. Note that this failure of FSSH on the electronic population in itself is reasonably well known. In the context of Tully's model #2, several research groups have shown that FSSH fails for low momentum when there are multiple crossing points.[1,34] That being said, as predicted by Shenvi et al.,[34] a phase-corrected FSSH can yield excellent agreement with the exact results for population and momentum; phase-corrected FSSH strongly outperforms both standard FSSH and Ehrenfest dynamics. Altogether, Figure 6 might lead one to

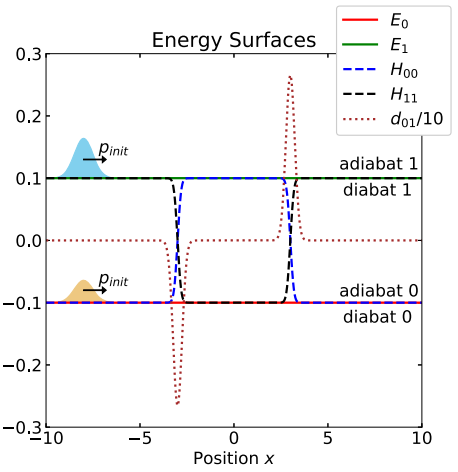


Figure 5. Energy surfaces for model 2 (i.e., the Hamiltonian in eq 9). Here, $A = 0.10$, $B = 3.0$, $C = 3.0$. The solid lines are the adiabatic surfaces. The dashed lines are the diabatic surfaces. The dotted line is the derivative coupling d_{01}. The initial Gaussian wave packets are plotted schematically with $x_{\text{init}} = -8.0$, $c_0 = 0.6$, $c_1 = 0.8$, and $\sigma = 1.0$.

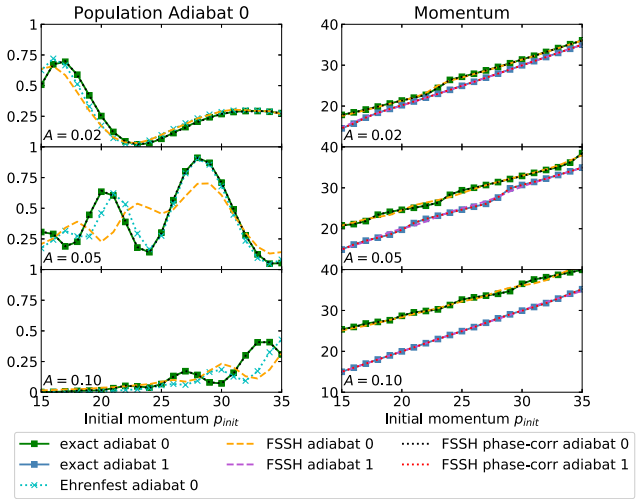


Figure 6. Same as Figure 2, but now for model 2. Left: population distribution on adiabat 0 after scattering as a function of initial momentum, p_{init}. Here, we include Ehrenfest data as well. Right: the momentum on adiabatic surfaces as a function of p_{init}. Initially, $c_1^2 = 1$. Note that phase-corrected FSSH can recover the correct electronic population, whereas both standard FSSH and Ehrenfest dynamics fail. Both FSSH and phase-corrected FSSH are able to capture the correct momentum on each adiabatic surface.

believe that the phase problem can be largely eliminated using a phase correction.

However, as can be seen in Figure 7, when the system is initialized with a superposition state, the phase correction in eq 3 clearly cannot fully fix all of the FSSH errors. Whereas phase-corrected FSSH can successfully recover the correct electronic population just as in Figure 3, the algorithm still fails to predict the correct momentum. Thus, while the phase correction of ref 34 is important, there is clearly a deeper recoherence problem within FSSH that ref 34 simply cannot fix.

Finally, in Figure 8, we plot the average results again (just as in Figure 4). We find that Ehrenfest dynamics now produces a large error in momentum when A is large (though still smaller than the FSSH error).

DOI: 10.1021/acs.jpca.9b03188
J. Phys. Chem. A 2019, 123, 5428−5435

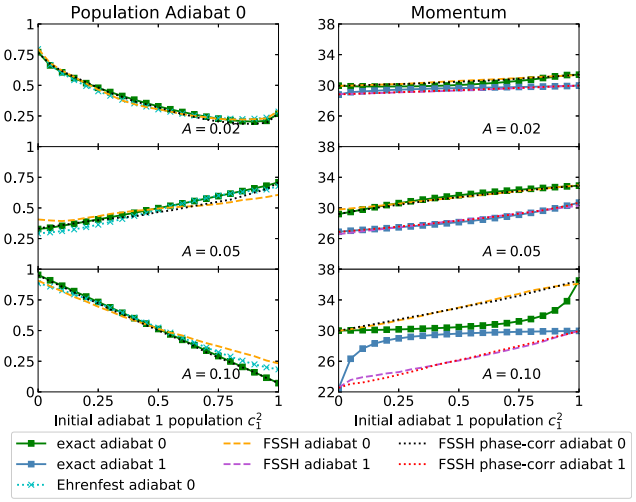


Figure 7. Same as Figure 3, but now for model 2. Left: population distribution on adiabat 0 after scattering as a function of initial superposition factor, c_1^2. Right: the momentum on adiabatic surfaces as a function of c_1^2. The initial momentum is $p_{init} = 30$. Note that, as in Figure 6, phase-corrected FSSH strongly outperforms standard FSSH for electronic populations. Nevertheless, neither algorithm can recover the correct momentum distribution when $c_1^2 \neq 1.0$, i.e., when one initializes dynamics on a superposition state. The accuracy of Ehrenfest dynamics as far as electronic population lies in between standard FSSH and phase-corrected FSSH.

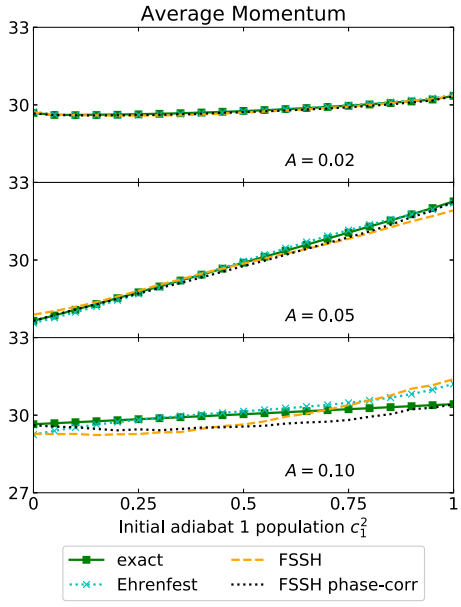


Figure 8. Same as Figure 4, but now for model 2. The average momentum over all trajectories as a function of c_1^2. The initial momentum is $p_{init} = 30$. Note that, for this case, Ehrenfest dynamics again outperforms FSSH (but the differences are now much smaller than in Figure 4).

4. DISCUSSION

4.1. Time Locality and the Minimum Hop Assumption. Based on the results above, we can clearly see the failure of FSSH: when A is large (in eq 7 or eq 9), the FSSH algorithm cannot predict the correct momentum when starting in a superposition state. And yet, FSSH clearly does perform correctly when the initial state is on a single adiabat, as found in the edges of Figures 3 and 7 (i.e., $c_1^2 = 0$ or 1). However, for both models, as the initial c_1^2 is tuned from 0 to 1, the momentum predicted by FSSH changes linearly, which disagrees with exact quantum dynamics. The phase-corrected version of FSSH[34] cannot solve this problem: phase correction leads to accurate electronic populations, but the momentum is still wrong. Apparently, the root of the problem is the well-known fact that FSSH cannot fully capture the recoherence: when two wave packets moving along different adiabats merge in the coupling region, the FSSH algorithm does not know how they should interfere exactly. And thus, several questions inevitably arise: when exactly is recoherence a problem for FSSH? Why does FSSH perform poorly for $A = 0.10$ (i.e., closer to the adiabatic limit) but not for $A = 0.02$ and 0.05 (i.e., closer to the nonadiabatic limit)?

To investigate this issue further, we list the hopping statistics for model 1 FSSH and model 2 phase-corrected FSSH in Tables 1 and 2, respectively. As shown in the tables, the percentage of multiple-hop trajectories increases when A is tuned from 0.02 to 0.10. The relatively large percentage of multiple-hop trajectories in the case of $c_1^2 = 0.5$ (compared against $c_1^2 = 1$ case) indicates that as the percentage of trajectories that experience multiple hops increases, FSSH tends to predict erroneous momentum distributions as the multiple hops disturb the phase accumulated between wave packets on different adiabats. There is one exception, i.e., when $A = 0.05$ in model 2, the percentage of trajectories with $N_{hop} = 3$ is larger, then $c_1^2 = 1$ (and smaller when $c_1^2 = 0.5$). Notice, however, that if we consider the number of trajectories with $N_{hop} \geq 4$, then $c_1^2 = 0.5$ does have a higher percentage of "multiple-hop trajectories" than $c_1^2 = 1$.

In a sense, we appear to have found something ironic: FSSH has too many hops back and forth and cannot be considered a "truly fewest switches" dynamic protocol. And given the data in Tables 1 and 2, we are led to believe that, in order for FSSH to recover the correct momentum results, we should seek a different algorithm with a truly minimal hopping rate, whereby redundant hops are eliminated from the standard FSSH. For trajectories in such an algorithm, when applied to the flat adiabats in models 1 and 2, trajectories that end up on the same adiabat as they began (and effectively do not hop) should keep their initial velocities, while trajectories that switch adiabats (and effectively hop once) should adjust velocities. The crucial question is then: what should we choose for these hopping probabilities if we must go beyond FSSH? While extracting the optimal hopping probabilities may not be feasible if we restrict ourselves to independent trajectories, let us assume we have access to all of the FSSH data: that is, we assume that trajectories are no longer independent—they talk to each other, and a hopping event for a single trajectory is decided by data from all trajectories (similar in spirit to ref 39).

To calculate the average momentum on each adiabat, we will separately treat the two distinct groups of trajectories, those that begin on one adiabat and end up on the same adiabat and those that begin on one adiabat and end up on the other adiabat. If the initial state is prepared with n_j^{init} population on adiabat j, for trajectories initialized on active adiabat state j, we denote the probability of hopping to adiabat k as $P_{j\to k}$. For those same trajectories, we denote the average momentum as $\langle p_{j\to k}\rangle$. With these definitions, if one considers the classical probability theory, one would predict that the final average momentum would be

DOI: 10.1021/acs.jpca.9b03188
J. Phys. Chem. A 2019, 123, 5428−5435

Table 1. Hopping Statistics for Trajectories with FSSH Dynamics (Model 1)[a]

c_1^2	A	N_{hop} = 0 (%)	N_{hop} = 1 (%)	N_{hop} = 2 (%)	N_{hop} = 3 (%)	N_{hop} = 4 (%)
1	0.02	8.46	90.23	1.31	0.00	0.00
1	0.05	37.77	52.64	9.59	0.00	0.00
1	0.1	75.10	10.91	13.98	0.01	0.00
0.5	0.02	37.25	45.12	17.63	0.00	0.00
0.5	0.05	33.25	48.98	17.65	0.12	0.00
0.5	0.1	31.86	44.21	20.78	2.94	0.21

[a]Initial condition: p_{init}^{x} = 30. Note that, when A increases, the probability for multiple hopping events increases.

Table 2. Hopping Statistics for Trajectories with Phase-Corrected FSSH Dynamics (Model 2)[a]

c_1^2	A	N_{hop} = 0 (%)	N_{hop} = 1 (%)	N_{hop} = 2 (%)	N_{hop} = 3 (%)	N_{hop} = 4 (%)	N_{hop} = 5 (%)	N_{hop} = 6 (%)
1	0.02	3.65	26.66	68.95	0.24	0.50	0.00	0.00
1	0.05	10.75	38.55	18.21	32.45	0.02	0.02	0.00
1	0.1	50.46	5.90	37.36	1.28	4.97	0.03	0.00
0.5	0.02	12.08	37.74	34.86	9.63	5.69	0.00	0.00
0.5	0.05	18.87	32.71	31.65	13.01	3.68	0.08	0.00
0.5	0.1	10.95	28.45	32.88	19.71	6.50	1.28	0.23

[a]Initial condition: p_{init}^{x} = 30. Note that, when A increases, the probability for multiple hopping events almost always increases.

$$\langle p_k \rangle = \frac{\sum_j n_j^{init} P_{j\to k} \langle p_{j\to k} \rangle}{\sum_j n_j^{init} P_{j\to k}} \tag{10}$$

In practice, for our simulations of model Hamiltonians (eqs 7 and 9), $P_{j\to k}$ and $\langle p_{j\to k} \rangle$ can be approximated by inspecting results where trajectories are initially prepared with n_j^{init} = 1 such that

$$P_{j\to k} \approx \langle n_k^{end} \rangle|_{n_j^{init}=1}$$
$$\langle p_{j\to k} \rangle \approx \langle p_k \rangle|_{n_j^{init}=1} \tag{11}$$

The results of the approximations in eq 11 are plotted in Figure 9. For both models 1 and 2, our predicted results are in excellent agreement with the exact results, suggesting that a nonlocal truly minimal hopping approximation without redundant hops can indeed fix the erroneous FSSH momentum distributions, Figures 3 and 7, as resulting from the recoherence problem.

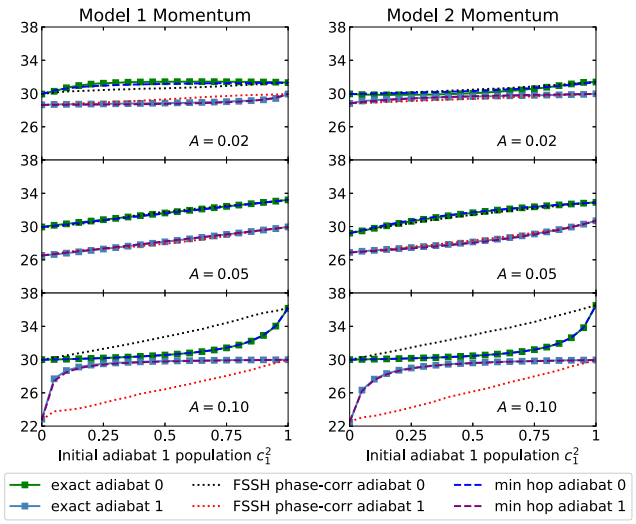


Figure 9. Momentum on the adiabatic surfaces as a function of c_1^2. Left: model 1. Right: model 2. The global minimum hop assumption (eq 10) correctly predicts the momentum distribution, especially for the case of large A.

5. CONCLUSIONS

To summarize, we have revisited the FSSH algorithm for two model systems where recoherence problems can emerge. We conclude that, when recoherence is important, FSSH cannot capture either the correct population or the momentum distribution. Adding a phase correction does improve the accuracy of FSSH as far as the electronic population, but momenta are still inaccurate. The root of the problem is that, because FSSH trajectories are propagated independently using only time-local information, these trajectories hop back and forth between surfaces too often. For the model problems we investigate here, the nonlocal minimal hopping assumption works much better as far as momentum distributions, and yet, this model is apparently time nonlocal and requires interaction between different trajectories. Thus, implementing such a truly, globally minimal hopping ansatz would be very hard (if not impossible) within the context of ab initio modeling.

Looking forward, there are three options. First, one can just accept that FSSH has limitations, work within the confines of those limitations for practical calculations, and, when possible, work with more rigorous dynamical approaches. Second, if one does not care about branching, one can employ Ehrenfest dynamics, which outperforms FSSH as far as calculating average observables after recoherence. However, note that, for many experiments in photochemistry and/or at surfaces, the adiabatic forces for different electronic states will be large and will lead to wave packets separating (i.e., branching), and so, Ehrenfest dynamics will fail. In the present draft, of course, we have focused exclusively on the case of particles with large initial velocities, where branching is not important, but, in general, running reliable Ehrenfest dynamics must inevitably require either introducing decoherence and branching[20,21,28,40,41] or potentially using clever tricks to include zero-point energy and bin the results.[42−44] Third, one can wonder if there is still room for FSSH improvement: can one further minimize hopping probabilities? From our perspective, working with interacting trajectories is computationally impossible for high-dimensional systems, and so, the more

DOI: 10.1021/acs.jpca.9b03188
J. Phys. Chem. A 2019, 123, 5428−5435

precise question that must be posed is this: can one improve upon FSSH and reduce the number of hops in a stable fashion with independent trajectories,[45] perhaps using time-nonlocal dynamics (perhaps in the spirit of Truhlar's time-uncertainty FSSH[46] or ab initio multiple spawning trajectories that have some memory[47,48])? Only time will tell.

AUTHOR INFORMATION

Corresponding Author

*E-mail: gaohan@sas.upenn.edu.

ORCID

Gaohan Miao: 0000-0002-6377-0614

Notes

The authors declare no competing financial interest.

ACKNOWLEDGMENTS

This material is based upon the work supported by the (U.S.) Air Force Office of Scientific Research (USAFOSR) award under AFOSR Grant no. FA9550-18-1-0497. J.S. acknowledges a David and Lucille Packard Fellowship.

ADDITIONAL NOTE

[a]Note in eq 5, $\langle\psi_k|\partial_x H|\psi_j\rangle$ is different from $\partial_x H_{kj} = \partial_x\langle\psi_k|H|\psi_j\rangle$.

REFERENCES

(1) Tully, J. C. Molecular Dynamics with Electronic Transitions. *J. Chem. Phys.* **1990**, *93*, 1061−1071.

(2) Oberhofer, H.; Reuter, K.; Blumberger, J. Charge Transport in Molecular Materials: An Assessment of Computational Methods. *Chem. Rev.* **2017**, *117*, 10319−10357.

(3) Habenicht, B. F.; Prezhdo, O. V. Nonradiative Quenching of Fluorescence in a Semiconducting Carbon Nanotube: A Time-Domain Ab Initio Study. *Phys. Rev. Lett.* **2008**, *100*, No. 197402.

(4) Nelson, T.; Fernandez-Alberti, S.; Chernyak, V.; Roitberg, A. E.; Tretiak, S. Nonadiabatic Excited-State Molecular Dynamics Modeling of Photoinduced Dynamics in Conjugated Molecules. *J. Phys. Chem. B* **2011**, *115*, 5402−5414.

(5) Sterpone, F.; Bedard-Hearn, M. J.; Rossky, P. J. Nonadiabatic Mixed Quantum-Classical Dynamic Simulation of π-Stacked Oligophenylenevinylenes. *J. Phys. Chem. A* **2009**, *113*, 3427−3430.

(6) Nelson, T.; Fernandez-Alberti, S.; Roitberg, A. E.; Tretiak, S. Nonadiabatic Excited-State Molecular Dynamics: Modeling Photophysics in Organic Conjugated Materials. *Acc. Chem. Res.* **2014**, *47*, 1155−1164.

(7) Fang, J.-Y.; Hammes-Schiffer, S. Comparison of Surface Hopping and Mean Field Approaches for Model Proton Transfer Reactions. *J. Chem. Phys.* **1999**, *110*, 11166−11175.

(8) Schwerdtfeger, C. A.; Soudackov, A. V.; Hammes-Schiffer, S. Nonadiabatic Dynamics of Electron Transfer in Solution: Explicit and Implicit Solvent Treatments That Include Multiple Relaxation Time Scales. *J. Chem. Phys.* **2014**, *140*, No. 034113.

(9) Subotnik, J. E.; Jain, A.; Landry, B.; Petit, A.; Ouyang, W.; Bellonzi, N. Understanding the Surface Hopping View of Electronic Transitions and Decoherence. *Annu. Rev. Phys. Chem.* **2016**, *67*, 387−417.

(10) Goyal, P.; Schwerdtfeger, C. A.; Soudackov, A. V.; Hammes-Schiffer, S. Nonadiabatic Dynamics of Photoinduced Proton-Coupled Electron Transfer in a Solvated Phenol−Amine Complex. *J. Phys. Chem. B* **2015**, *119*, 2758−2768.

(11) Goyal, P.; Schwerdtfeger, C. A.; Soudackov, A. V.; Hammes-Schiffer, S. Proton Quantization and Vibrational Relaxation in Nonadiabatic Dynamics of Photoinduced Proton-Coupled Electron Transfer in a Solvated Phenol-Amine Complex. *J. Phys. Chem. B* **2016**, *120*, 2407−2417.

(12) Landry, B. R.; Subotnik, J. E. Quantifying the Lifetime of Triplet Energy Transfer Processes in Organic Chromophores: A Case Study of 4-(2-Naphthylmethyl) Benzaldehyde. *J. Chem. Theory Comput.* **2014**, *10*, 4253−4263.

(13) Jain, A.; Subotnik, J. E. Surface Hopping, Transition State Theory, and Decoherence. II. Thermal Rate Constants and Detailed Balance. *J. Chem. Phys.* **2015**, *143*, No. 134107.

(14) Parandekar, P. V.; Tully, J. C. Mixed Quantum-Classical Equilibrium. *J. Chem. Phys.* **2005**, *122*, No. 094102.

(15) Jain, A.; Alguire, E.; Subotnik, J. E. An Efficient, Augmented Surface Hopping Algorithm That Includes Decoherence for Use in Large-Scale Simulations. *J. Chem. Theory Comput.* **2016**, *12*, 5256−5268.

(16) Barbatti, M.; Granucci, G.; Persico, M.; Ruckenbauer, M.; Vazdar, M.; Eckert-Maksić, M.; Lischka, H. The on-the-Fly Surface-Hopping Program System Newton-X: Application to Ab Initio Simulation of the Nonadiabatic Photodynamics of Benchmark Systems. *J. Photochem. Photobiol., A* **2007**, *190*, 228−240.

(17) Bittner, E. R.; Rossky, P. J. Quantum Decoherence in Mixed Quantum-Classical Systems: Nonadiabatic Processes. *J. Chem. Phys.* **1995**, *103*, 8130−8143.

(18) Schwartz, B. J.; Bittner, E. R.; Prezhdo, O. V.; Rossky, P. J. Quantum Decoherence and the Isotope Effect in Condensed Phase Nonadiabatic Molecular Dynamics Simulations. *J. Chem. Phys.* **1996**, *104*, 5942−5955.

(19) Prezhdo, O. V.; Rossky, P. J. Evaluation of Quantum Transition Rates from Quantum-Classical Molecular Dynamics Simulations. *J. Chem. Phys.* **1997**, *107*, 5863−5878.

(20) Hack, M. D.; Truhlar, D. G. Electronically Nonadiabatic Trajectories: Continuous Surface Switching II. *J. Chem. Phys.* **2001**, *114*, 2894−2902.

(21) Volobuev, Y. L.; Hack, M. D.; Topaler, M. S.; Truhlar, D. G. Continuous Surface Switching: An Improved Time-Dependent Self-Consistent-Field Method for Nonadiabatic Dynamics. *J. Chem. Phys.* **2000**, *112*, 9716−9726.

(22) Jasper, A. W.; Truhlar, D. G. Electronic Decoherence Time for Non-Born-Oppenheimer Trajectories. *J. Chem. Phys.* **2005**, *123*, No. 064103.

(23) Jasper, A. W.; Truhlar, D. G. Non-Born-Oppenheimer molecular dynamics of Na···FH photodissociation. *J. Chem. Phys.* **2007**, *127*, No. 194306.

(24) Fang, J.-Y.; Hammes-Schiffer, S. Improvement of the Internal Consistency in Trajectory Surface Hopping. *J. Phys. Chem. A* **1999**, *103*, 9399−9407.

(25) Horenko, I.; Salzmann, C.; Schmidt, B.; Schütte, C. Quantum-Classical Liouville Approach to Molecular Dynamics: Surface Hopping Gaussian Phase-Space Packets. *J. Chem. Phys.* **2002**, *117*, 11075−11088.

(26) Subotnik, J. E.; Shenvi, N. Decoherence and Surface Hopping: When Can Averaging Over Initial Conditions Help Capture the Effects of Wave Packet Separation? *J. Chem. Phys.* **2011**, *134*, No. 244114.

(27) Wang, L.; Akimov, A.; Prezhdo, O. V. Recent Progress in Surface Hopping: 2011−2015. *J. Phys. Chem. Lett.* **2016**, *7*, 2100−2112.

(28) Prezhdo, O. V.; Rossky, P. J. Mean-Field Molecular Dynamics with Surface Hopping. *J. Chem. Phys.* **1997**, *107*, 825−834.

(29) Kapral, R. Surface Hopping from the Perspective of Quantum−Classical Liouville Dynamics. *Chem. Phys.* **2016**, *481*, 77−83.

(30) Subotnik, J. E.; Ouyang, W.; Landry, B. R. Can We Derive Tully's Surface-Hopping Algorithm from the Semiclassical Quantum Liouville Equation? Almost, but Only with Decoherence. *J. Chem. Phys.* **2013**, *139*, No. 214107.

(31) Kelly, A.; Markland, T. E. Efficient and Accurate Surface Hopping for Long Time Nonadiabatic Quantum Dynamics. *J. Chem. Phys.* **2013**, *139*, No. 014104.

(32) Petit, A. S.; Subotnik, J. E. How to Calculate Linear Absorption Spectra with Lifetime Broadening Using Fewest Switches Surface Hopping Trajectories: A Simple Generalization of Ground-State Kubo Theory. *J. Chem. Phys.* **2014**, *141*, No. 014107.

DOI: 10.1021/acs.jpca.9b03188
J. Phys. Chem. A 2019, 123, 5428−5435

(33) Bellonzi, N.; Jain, A.; Subotnik, J. E. An Assessment of Mean-Field Mixed Semiclassical Approaches: Equilibrium Populations and Algorithm Stability. *J. Chem. Phys.* **2016**, *144*, No. 154110.
(34) Shenvi, N.; Subotnik, J. E.; Yang, W. Phase-Corrected Surface Hopping: Correcting the Phase Evolution of the Electronic Wavefunction. *J. Chem. Phys.* **2011**, *135*, No. 024101.
(35) Shenvi, N.; Roy, S.; Tully, J. C. Dynamical Steering and Electronic Excitation in NO Scattering from a Gold Surface. *Science* **2009**, *326*, 829−832.
(36) Jasper, A. W.; Truhlar, D. G. Improved Treatment of Momentum at Classically Forbidden Electronic Transitions in Trajectory Surface Hopping Calculations. *Chem. Phys. Lett.* **2003**, *369*, 60−67.
(37) Shenvi, N.; Yang, W. Achieving Partial Decoherence in Surface Hopping Through Phase Correction. *J. Chem. Phys.* **2012**, *137*, No. 22A528.
(38) Kosloff, D.; Kosloff, R. A Fourier Method Solution for the Time Dependent Schrödinger Equation as a Tool in Molecular Dynamics. *J. Comput. Phys.* **1983**, *52*, 35−53.
(39) Martens, C. C. Surface Hopping by Consensus. *J. Phys. Chem. Lett.* **2016**, *7*, 2610−2615.
(40) Bedard-Hearn, M. J.; Larsen, R. E.; Schwartz, B. J. Mean-Field Dynamics with Stochastic Decoherence (MF-SD): A New Algorithm for Nonadiabatic Mixed Quantum/Classical Molecular-Dynamics Simulations with Nuclear-Induced Decoherence. *J. Chem. Phys.* **2005**, *123*, No. 234106.
(41) Subotnik, J. E. Augmented Ehrenfest Dynamics Yields a Rate for Surface Hopping. *J. Chem. Phys.* **2010**, *132*, No. 134112.
(42) Cotton, S. J.; Miller, W. H. Symmetrical Windowing for Quantum States in Quasi-Classical Trajectory Simulations: Application to Electronically Non-Adiabatic Processes. *J. Chem. Phys.* **2013**, *139*, No. 234112.
(43) Cotton, S. J.; Miller, W. H. Symmetrical Windowing for Quantum States in Quasi-Classical Trajectory Simulations. *J. Phys. Chem. A* **2013**, *117*, 7190−7194.
(44) Cotton, S. J.; Miller, W. H. A Symmetrical Quasi-Classical Spin-Mapping Model for the Electronic Degrees of Freedom in Non-Adiabatic Processes. *J. Phys. Chem. A* **2015**, *119*, 12138−12145.
(45) Martens, C. C. Surface Hopping without Momentum Jumps: A Quantum-Trajectory-Based Approach to Nonadiabatic Dynamics. *J. Phys. Chem. A* **2019**, *123*, 1110−1128.
(46) Jasper, A. W.; Stechmann, S. N.; Truhlar, D. G. Fewest-Switches with Time Uncertainty: A Modified Trajectory Surface-Hopping Algorithm with Better Accuracy for Classically Forbidden Electronic Transitions. *J. Chem. Phys.* **2002**, *116*, 5424−5431.
(47) Martínez, T. J.; Ben-Nun, M.; Levine, R. D. Multi-Electronic-State Molecular Dynamics: A Wave Function Approach with Applications. *J. Phys. Chem.* **1996**, *100*, 7884−7895.
(48) Ben-Nun, M.; Quenneville, J.; Martínez, T. J. Ab Initio Multiple Spawning: Photochemistry from First Principles Quantum Molecular Dynamics. *J. Phys. Chem. A* **2000**, *104*, 5161−5175.

DOI: 10.1021/acs.jpca.9b03188
J. Phys. Chem. A 2019, 123, 5428−5435